Development of Scintillator-Based Muon Detectors for Muography

Jacques Marteau, Jean de Bremond d'Ars, B. Carlus, A. Chevalier, A. Cohu, T. Descombes, D. Gibert, K. Jourde, B. Kergosien, N. Lesparre, et al.

Development of Scintillator-Based Muon Detectors for Muography

Jacques Marteau[1,2], Jean de Bremond d'Ars[3], Bruno Carlus[1], Antoine Chevalier[1], Amélie Cohu[1], Thierry Descombes[4], Dominique Gibert[5,6], Jean-Christophe Ianigro[1], Kevin Jourde[7], Bruno Kergosien[3], Nolwenn Lesparre[8], Jean-Luc Montorio[1], and Marina Rosas-Carbajal[9]

[1]Institute of Physics of the 2 Infinities, Joint Research Unit (UMR 5822), CNRS/IN2P3, University Claude Bernard Lyon 1, Villeurbanne, France

[2]International Virtual Muography Institute, Global

[3]Géosciences Rennes, Joint Research Unit (UMR 6118), CNRS and University of Rennes, Rennes, France

[4]Laboratory for Subatomics Physics and Cosmology, Université Grenoble Alpes, Grenoble, France

[5]Laboratory of Geology of Lyon: Earth, Planets and Environments, University of Lyon, Villeurbanne, France

[6]National Volcano Observatory Service, University of Lyon, Villeurbanne, France

[7]French Alternative Energies and Atomic Energy Commission (CEA), Grenoble, France

[8]Laboratory of Hydrology and Geochemistry of Strasbourg, Strasbourg University, Strasbourg, France

[9]University of Paris, Institute of Earth Physics of Paris (IPGP), CNRS, Paris, France

ABSTRACT

In this chapter, we describe basic features and give some current applications of the most popular detection technology used in muography: the scintillator-based muon detectors, widely used not only in volcanology, where their properties find natural applications, but also in geosciences, archeology, non-invasive industrial control, civil engineering, homeland security, nuclear non-proliferation and more. As we will emphasize in the following sections, there are many advantages in the use of scintillators, which are known to be robust – and therefore usable in harsh environmental conditions – and offer real-time analogic measurement capabilities with a good space and time resolution. The design of such detectors is flexible and may be used in many different ways depending on the target under study, the field conditions, the modularity of the detectors etc. Throughout this chapter, we will focus on one particular muon detector (also referred to as "muon telescope") originally designed to study the active volcanic dome of the Soufrière of Guadeloupe to show the generic features of this detection technique.

17.1. INTRODUCTION

From the early investigations that Alvarez performed in the Egyptian Chephren (Alvarez et al., 1970) to the recent results of the ScanPyramids project (Morishima et al., 2017), muons have gained in popularity not only in the archeology domain but also in geosciences in general, and now even among industries. Muons are elementary particles and usually belong to the "high energy physics" (HEP) scientific world, with projects like one of the largest experiments ever built, the LHC at CERN (https://home.cern/fr) in Switzerland – the world's largest accelerator complex – or Super-Kamiokande in Japan (http://www-sk.icrr.u-tokyo.ac.jp/sk/index-e.html) – the world's largest underground detector. In this world, those particles are both the subjects of research and the tools with which to achieve this research.

Reduced and autonomous particle detectors have been designed and made available outside the world of HEPs, e.g., for medical imaging (Positron Emission Tomography, PET, systems using inorganic scintillators developed for calorimetry in the HEP experiments). Innovative techniques have been developed that use elementary particles not for themselves but as tools for interdisciplinary sciences. This is the case for muography.

But what type of technology? How does one detect elementary particles that no one sees or feels? Coming back to the early and recent archeological investigations in Egypt, there were very different detection techniques, with very different properties and sensitivities: "spark chambers" for Alvarez, and "nuclear emulsions," "plastic scintillators", and "micromegas" for the ScanPyramids project.

The choice among different technologies is driven by many criteria, depending on the access to a given knowledge, the performances required, the experimental conditions, the environmental context, the cost, the transportability, etc. This chapter presents the general features of one of the most popular detection techniques used in muon imaging: the scintillator-based detectors. The chapter is organized as follows. After a short presentation of the muon detection requirements and constraints (Section 17.2), a detailed description is given on one particular scintillator-based detector's design used in volcanology (Section 17.3). Then we review different past and present projects using this technology (Section 17.4), and finally we show "typical" applications recently achieved an overview of the scintillator-based detector's interesting power.

17.2. DETECTING MUONS: DIRECT AND INVERSE PROBLEM

Muon imaging has emerged as a powerful method to complement standard tools in Earth sciences. The general features of this technique – the muography – are reviewed elsewhere in this book. We recall that atmospheric muons represent the largest proportion of charged particles reaching the surface of the Earth, and that they are secondary products of cosmic-ray interactions with the atmosphere. Their penetrating power into ordinary matter makes them an ideal probe of large and dense structures that one would like to scan. At the same time, their sensitivity to the atmospheric conditions in which they are produced may provide valuable information on some not-so easily accessible parameters such as, e.g., the temperature at the top of the stratosphere. Therefore the range of applications of muography may be very large, one of the main reasons for today's domain expansion. Muography techniques is usually split into two different modes: "absorption muography" and "scattering muography." This chapter will deal essentially with the absorption mode, which proceeds like X-ray medical imaging: the mass distributions inside a given target are inferred from the measurement of the reduced muon flux due to their interaction with the matter of the target.

The starting point for muography is of course the detection of the muons to feed the so-called "direct problem" of the target's imaging with data. This detection is quite simple, since atmospheric muons are charged leptons. For a general review on muon properties, see the Particle Data Group data compilation (https://pdg.lbl.gov/2020/tables/rpp2020-sum-leptons.pdf). As they cross matter, they will interact with the charges of the medium and lose a fraction of their total energy. Atmospheric muons at ground level have an average energy usually ranging close to the minimum of ionization (Gaisser et al., 2016). For a more general review on the properties of particles through matter, see the Particle Data Group (https://pdg.lbl.gov/2020/reviews/rpp2020-rev-passage-particles-matter.pdf). This energy loss may be converted into various types of signals: charge avalanches in gaseous detectors such as resistive plate chambers (RPC) or Micro-Megas; silver atoms in nuclear photographic emulsions; or photons in scintillation detectors. The various detection devices mentioned are described in other chapters, while we will focus on the "scintillator-based" detectors.

Note that the fraction of energy lost by the particles is usually small in the so-called "tracking detectors," while it should be large in the "calorimeters" where one wants to measure the total energy of the particles. The collection of these signals down to the readout electronics (usually called "front-end electronics") and then to the data acquisition (DAQ) and back-end systems (embedded CPU or electronic racks) allows us to store the information of the muons' passage through the detector: position and time of the hit, plus additional data in certain systems, like, e.g., the energy deposited,

the particle's energy or momentum, etc. Details on detection techniques, particle interaction with matter, and high-energy physics experimental techniques are found in Leo (1987).
The minimal requirements for the detection devices used for muography are therefore the tracking capabilities, i.e., the possibility to reconstruct the trajectory of the crossing particles – which corresponds to their incident direction if one neglects the scattering effects induced by the detector itself. After the track reconstruction one is able either to count the number of muons recorded in a given direction and compare to some models (absorption mode), or to count the number of deviated trajectories after the crossing of a target (scattering mode). The tracking performances are measured in terms of spatial (and/or angular) resolution, usually driven by the size of the detector segmentations or pixels, and in terms of timing resolution.
Good spatial and angular resolutions are absolutely necessary if one wants to scan precisely details in rather small objects. These requirements are less stringent for large structures, such as volcanic domes where the measured fluxes are strongly reduced because of the target's opacity. For such measurements, the important parameter is the detector's acceptance, i.e., its capability of collecting the maximal number of muons for a given active surface (Sullivan, 1971). Larger matrices offer a larger detection area, which reduces the acquisition time for a given angular resolution (Lesparre et al., 2010).
Good timing performances are usually required for background reduction and time-of-flight measurements. The background rejection is important for outdoor applications where one needs to eliminate random coincidences of hits leading to fake tracks and to spurious "events". Therefore fine timestamps, of the order of the nanosecond or below, allow short time coincidence windows and maximal background rejection. As its name implies, time-of-flight measurement consists of measuring the time taken by the muon to cross the detector and discriminating whether it was propagating downwards or upwards. This technique is a very useful asset for background rejection, but requires sub-nanosecond timing resolution. And even better in the case of an event-by-event discrimination requirement.
We will see in the following section how the scintillation mechanism works and how it is used for muon detectors. But before this, we would like to insist on a general comment that applies to muography. The real difficulty of this technique is less the muon detection than the constraints on the so-called "inverse problem" when going from raw data to reconstructed mass distributions (Nagamine, 2003). Indeed, muography is not suited for standard imaging techniques that one can cross in medical imaging, like, for example, the radon transform. One of the main reasons is the poor statistics, limited by the natural atmospheric muon flux. Furthermore, a single muon detector in absorption mode will measure the attenuation of the muon flux integrated all over the path of the muons inside the target under study, i.e., its "opacity". To go from an "opacity" map to a "density" map requires a model, or more generally an "inversion technique" that provides the most probable mass distribution functions inside the target (Lesparre et al., 2010). The inverse problem needs to be constrained by the a priori information (in the Bayesian language) but also driven by the data quality. This imposes the requirements on the detector performance in terms of acceptance, resolution, stability in operation, duty cycle, etc. We will see in the following section how these requirements are fulfilled with plastic scintillators.

17.3. TECHNOLOGIES: DESIGN AND OPERATION OF SCINTILLATOR-BASED DETECTORS

17.3.1. State of the Art

Scintillators are well-known detectors widely used in HEP. They are integrated into trackers or into calorimeters. The scintillation of some materials results in the conversion of the deposited energy into photons (usually in the UV spectral range), which are then guided down to a photo-detector (Leo, 1987). There are many types of scintillators (liquid or solid, organic or inorganic) and many types of photodetectors (photo-diodes, avalanche photo-diodes, photo-transistors, photo-multipliers, hybrid photo-multipliers, "silicon" photo-multipliers, etc).

In the following section we will focus on plastic scintillators, which are polystyrene with adjuvants like PPO (2,5-diphenyloxazole) and POPOP (1,4-bis(5-phenyloxazole-2-yl)benzene) to generate the scintillation photons. The polystyrene may be molded or extruded in various shapes, which makes the designs of scintillator-based detectors very attractive because of their modularity. Indeed, one can arrange the total detection surface, the transverse segmentation, the light collection system, etc., according to the experimental needs and constraints. We will restrict designs where those photons are generated in a "bar" (of triangular or rectangular shape) and then readout directly by a photo-detector glued somehow to the bar or trapped into an wavelength shifting (WLS) fiber down to the photo-detector. The shifting in wavelength enables us to match the maximal detection efficiency spectrum of the photo-cathodes, e.g., the widely used bilalkali ones, usually peaked in the visible green region.
Apart from the advantage of the design's flexibility, the choice of scintillator option is also driven by the robustness of the plastic scintillators, which allow us to build light, low-cost detectors particularly well suited to field conditions and actually used for most studies on volcanoes (Lesparre et al., 2011; Tanaka et al., 2009). This will be exemplified in the following sections. Many collaborations exist among Earth science and (astro)particle institutes in the world, which vary in the design of the detector, the methodology used (absorption or scattering), and specific applications. We will present some of them in Section 17.4.
In the following, we focus on the muon detectors, sometimes also referred to as "muon telescopes", of the Diaphane collaboration, one of the first teams among the growing number of international teams now involved with muography techniques. Diaphane is a French interdisciplinary collaboration between particle physicists of the CNRS-IN2P3 institute (IP2I Lyon) and geophysicists of the CNRS-INSU institute (Géosciences Rennes, IPG Paris). It also involves their related universities (References and details in: https://diaphane-muons.com/). Since its foundation in 2009, the team is involved in all aspects of muography, including instrument design and construction, field experiments on volcanoes, underground tunnels, civil engineering and urban structures, industrial infrastructures and processing, modelling, data analysis and inversion. Some of the results obtained by the Diaphane teams are briefly presented in Section 17.5 and in other chapters of this book.

17.3.2. Muon Detectors as Field Instruments

The Diaphane detectors have been designed from the beginning to cope with the harshest conditions of the most demanding fields, such as the active dome of tropical volcanoes like the Soufrière of Guadeloupe, which has a relative humidity higher than 95%, heavy rains, and strong winds. There, most telescope locations are far from roads and power lines, and the total weight and power consumption must be low enough to allow both helicopter hauling and solar panel powering.
Examples of long-standing installations around the active dome are displayed in Fig. 17.1. The muon telescopes have been operated around this volcano for more than 10 years, and even during the recent hurricane periods (e.g., Maria in 2017). The global scheme of a scintillator-based detector is displayed in Fig. 17.2 along with the theoretical muon rays in the detector's acceptance. Those detectors are simply "XY trackers" where scintillator bars are grouped in a plane to arrange two orthogonal arrays per plane. The "event building" in such detector is quite straightforward: when a charged particle hits the detection planes, the X and Y bars where the energy has been deposited form the "pixel" crossed by the particle. The measurement of the hits timestamps in all the detection planes (at least three) and the association of those that are in coincidence give the coordinates (X,Y, plane number) of the particle's trajectory.
The challenges of the field operations imply constraining requirements such as:

1. The portability on hardly accessible rough terrains. This is usually achieved with a modular design of independent detection elements connected together on site. In this particular case, the detection planes, electronics control box, and mechanical frames are independent elements that one can bring separately.

2. The lowest possible power consumption, compatible with different outdoor electrical power sources (photovoltaic, wind turbine, fuel cell) to reduce power blackout in case of harsh environmental conditions (cloudy weather, ash fall, hurricanes).
3. Autonomous, auto-triggerable, and remotely accessible electronics readout systems that are compatible with long exposure times, imposed in the case of large structures scanning such as a volcanic dome.
4. The highest muon detection sensitivity to profit from a maximum of muons that manage to cross the target and reduce the time exposure.
5. The largest stability with time for the long-term monitoring of a target, e.g., the follow-up of the hydrothermal system of a volcanic dome.
6. Low cost overall design.

Figure 17.1 Two versions of muon telescopes operating on the Soufrière of Guadeloupe (Rocher Fendu location). The electrical power is provided by solar panels and a Wi-Fi link allows daily data download and software parameterization. The mechanical frames allow zenith/azimuth orientations

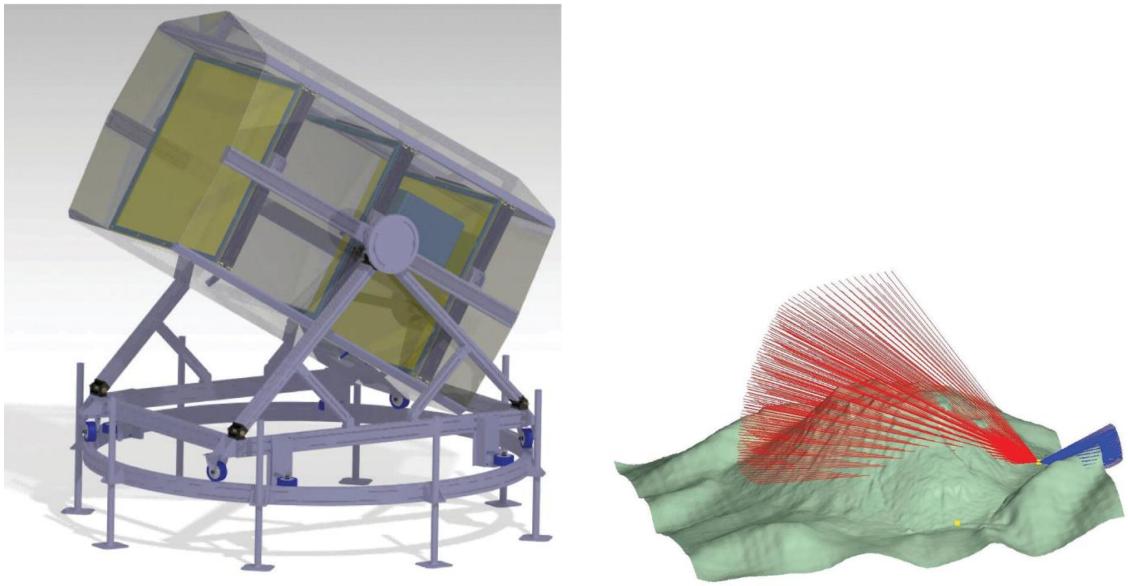

Figure 17.2 (Left) Schematics of a muon detector with three active planes (front, middle, and rear) protected by some tarpaulin. The mechanical frames are held by adjustable scaffolding feet to adjust the horizontality if needed. The central plane may be complemented with passive shielding (lead bricks, stainless steel plates, etc.) to absorb the low-energy component of the atmospheric flux. (Right) Representation of theoretical muon rays reaching the detector. The different lines of sight are defined

by the detector's pixelization. In red, the trajectories of the downwards propagating muons. In blue, the upwards ones (Lesparre et al., 2012).

17.3.3. An Example of Detailed Implementation

In this section we detail as a particular example one of the Diaphane detectors (more than 15 detectors have already been built and operated). As mentioned above, the sensitive part of the detectors is made of plastic scintillator, usually produced for various HEP projects such as long baseline neutrino experiments: the former MINOS (Main Injector Neutrino Oscillation Search) (Adamson, 2008) and OPERA (Oscillation Project with Emulsion- tRacking Apparatus) (Agafonova et al., 2010) experiments, and the current T2K (Tokai to Kamioka) (Abe et al., 2013) project in Japan, etc. For instance, the plastic scintillator produced in Fermilab is extruded with a central hole or machined to host a WLS fibre for scintillation light collection. It has been optimized in terms of light yield and attenuation (Pla-Dalmau et al., 2001). We also used scintillators produced by JINR in Russia. The scintillator bars have a rectangular cross-section of 1–5×0.5 to 1 cm2 depending on the applications and are co-extruded with a TiO2 reflective coating or recovered with highly reflective paint. The WLS optical fibres used (Kuraray Y11 or Bicron BCF 91A) have a 1–1.5 mm diameter, collect the UV scintillation light and re-emit the signal in the green range, where the photosensors have an optimal response, as shown in Fig. 17.3 (see also Lesparre et al., 2011, and references therein).

A fibre-to-pixel connection in ensured by an optical system, which is plugged into a pixelized photomultiplier (Hamamatsu 8804-300) with upgraded bialkali photo-cathode. Those photomultipliers (PMT) have 8×8 pixels, a typical gain of 106 with a factor 1:3 dispersion on the pixel gains. The relatively high gain requires moderate amplification, but the spread implies the necessity of a channel-to-channel gain correction. This is actually included in the present electronics of the telescopes. We also developed an electronic readout system for silicon photo-multipliers (Hamamatsu Multi-Pixel Photon Counter).

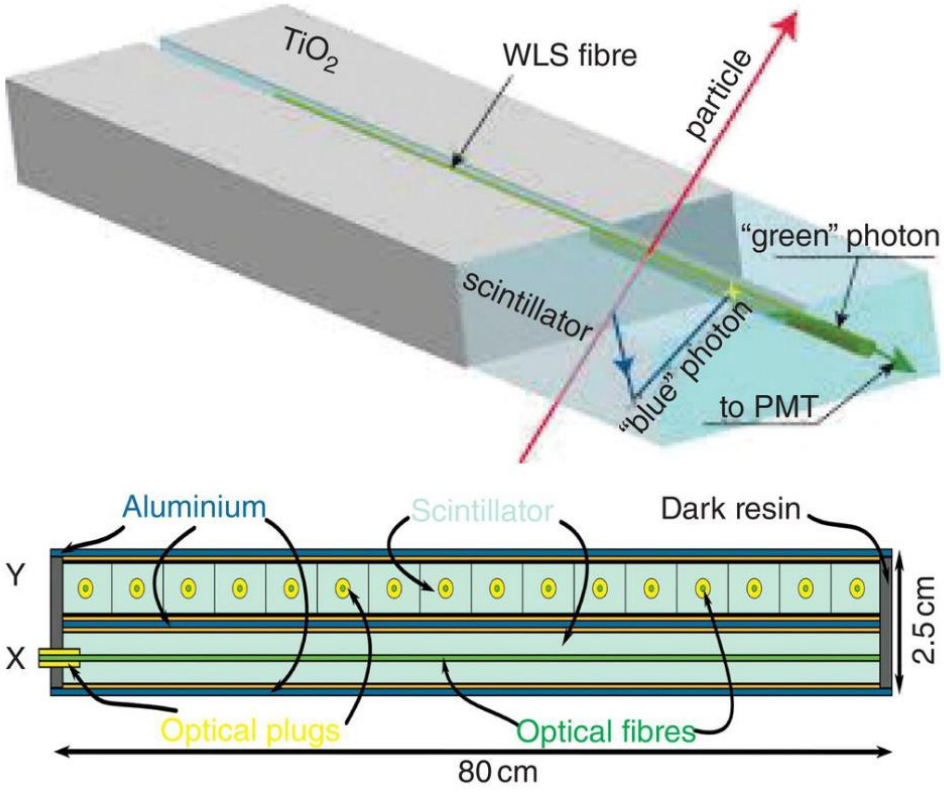

Figure 17.3 (Top) Detection principle of a scintillator+WLS fibre system. (Bottom) Cross-section view of a matrix with 16×16 pixels, an area of 0.8×0.8 = 0.64 m2 and one optical plug at one extremity of each bar (Lesparre et al., 2011).

The scintillator bars described above are aligned in the orthogonal X and Y directions to form a XY detection matrix (Figs. 17.3, 17.4, and 17.5), which may count 10×10, 16×16, or 32×32 pixels, according to the design. The transverse size of the bars defines of course the spatial and angular resolution of the detection system.

One telescope contains at least three matrices (Fig. 17.1) to define the trajectory of a detected particle from the pixels fired on each matrix. The third matrix is there to reduce the occurrence of fake tracks due to the possibility of random coincidences on two planes. The total aperture angle and the angular resolution of the telescope may be adjusted by changing the distance between the matrices. This technological choice is flexible and easily adaptable to the requirements of any experiment.

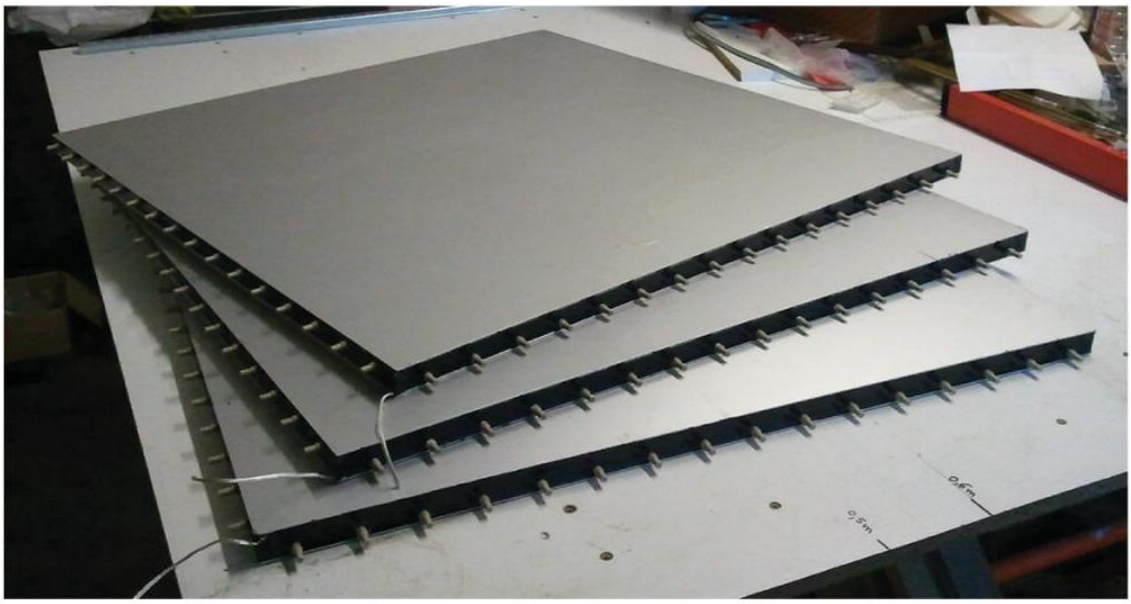

Figure 17.4 First-generation Scintillator matrices with 16×16 strips from Fermilab. The connections between WLS and clear fibers are individual.

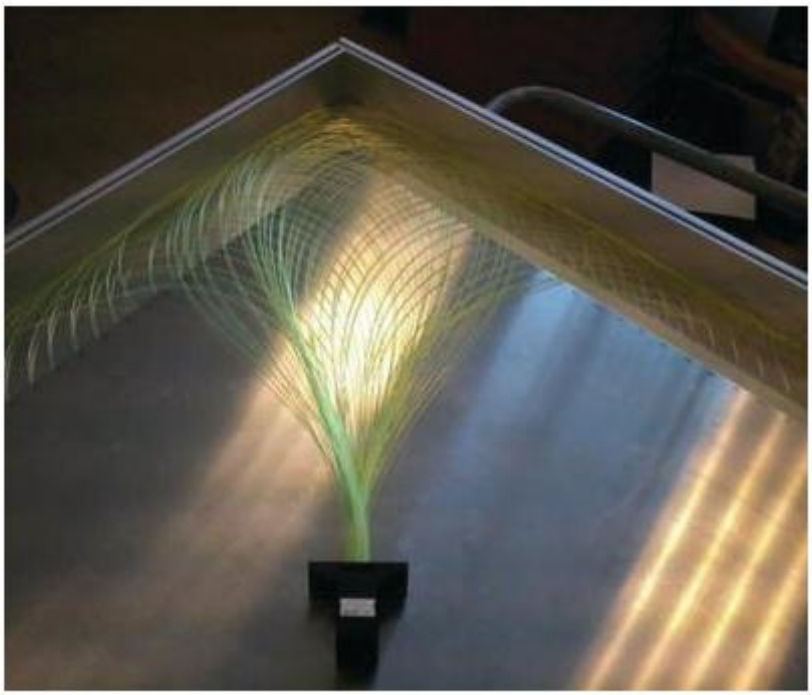

Figure 17.5 Second-generation scintillator matrices with 32×32 strips from JINR. The WLS fibers are directly connected to the MAPMT via an optical cookie.

All the readout electronics chains have been developed earlier at IP2I Lyon (patented system) for the OPERA experiment hosted in the Italian Gran Sasso laboratory. This experiment took data from 2006 to 2012 and signed the $\nu_\mu \rightarrow \nu_\tau$ oscillations in appearance mode (Agafonova et al., 2010). Using the OPERA electronics allowed us to speed up the production of the first telescope and to begin field experiments as soon as possible. This is a standard starting point for muography experiments as HEP "spin-off" projects. Indeed, the first telescope was available in less than a year and the first density radiography of the Soufrière of Guadeloupe was obtained in less than two years. The electronics scheme is based on the concept of "Ethernet capable smart autonomous sensors" with auto-triggerable front-end electronics, stand-alone configuration of the photo-detector, and electronics parameters and communication protocol through Ethernet. Figs. 17.6 and 17.7 show the readout systems for the PMT and SiPM, respectively. The DAQ system performs the detector configuration, the monitoring, the event building, and data transfer to the on-board computer (Marteau et al., 2012, 2014). The distributed client/server software is based on the CORBA standard (https://www.corba.org/) and allows continuous running, online filtering, data processing, and storage. A clock broadcasting system synchronizes all sensors with a common clock unit regulated by GPS.

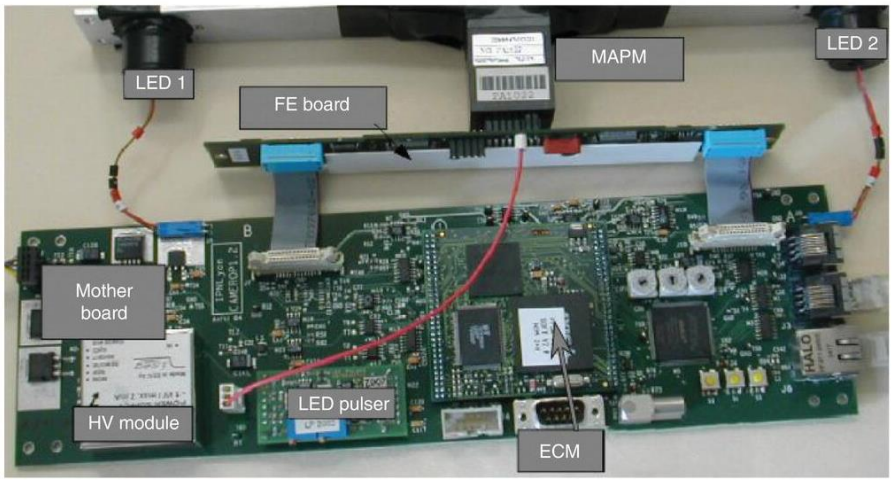

Figure 17.6 Readout system for MAPM. The front-end (FE) board, connecting the MAPM, has two multichannel chips for the trigger generation and the signal readout. The mother-board hosts the Ethernet Controller Module (ECM), the High Voltage (HV) module, the LED pulser system, and the clock readout devices (Lesparre et al., 2011).

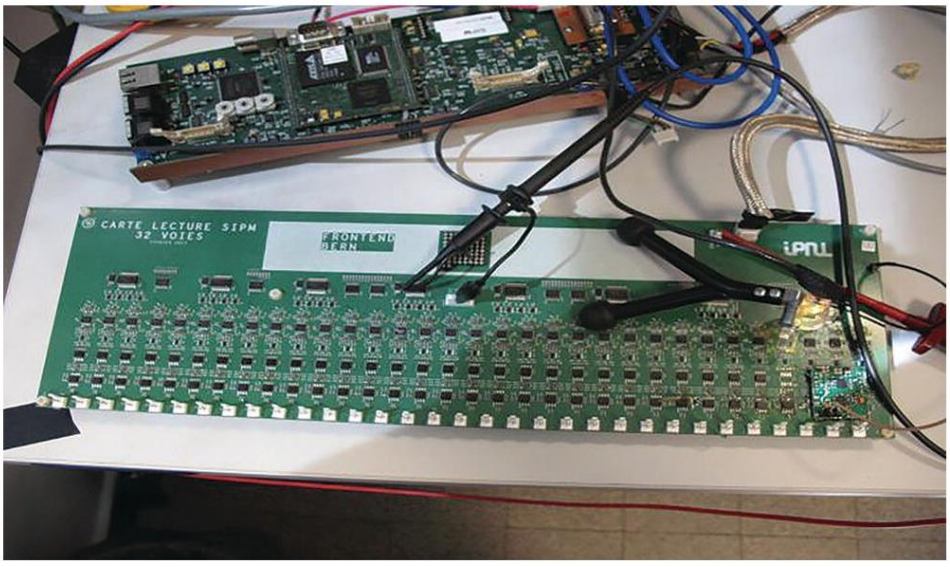

Figure 17.7 SiPM Trigger Board connected to the standard readout chain used in the Diaphane telescope.

This technology has proven to be adapted to the field conditions for which it has not been designed at all initially. In particular, the moderate power consumption complies with the drastic constraints of the solar panels. The original system was upgraded by the implementation, within the mezzanine processor boards, of a 100 picoseconds scale time-to-digital converter TDC (Marteau et al., 2014) allowing a global time-of-flight based background rejection as discussed earlier (Jourde et al., 2013).

17.3.4. Some Results in Volcanology with this Implementation

With the kind of detectors presented in Section 17.3.3, the Diaphane collaborators have been making continuous muography experiments for more than 10 years on different fields, one of those being the Soufrière of Guadeloupe volcano, in the Lesser Antilles, making this volcano the most equipped in the world with a network of 6 telescopes simultaneously taking data in the 2017–2020 period (Figs. 17.1, 17.8).

The data set acquired is unique and allowed us to study unknown or poorly studied phenomena and methods like:

1. the structural imaging of the dome from different points of view (Fig. 17.9) exhibiting the highly heterogeneous constitution of the dome;
2. the 3D density structure of a lava dome (Jourde et al., 2015a) and in complete coincidence with the 3D structure obtained with ERT techniques (Rosas-Carbajal et al., 2017);
3. the transfers of huge mass and energy associated with the hydrothermal activity (Jourde et al., 2016b; Le Gonidec et al., 2019);
4. the effect of upward flux of muons (Jourde et al., 2013);
5. the muon diffusion at the surface of the volcano (Gómez et al., 2017);
6. the joined muon-gravimetry inversion to perform 3D reconstruction of the dome (Jourde et al., 2015b); and
7. the combination measurements of muography and seismic noise data (Le Gonidec et al., 2019).

Besides their pure scientific interest, these results are of great importance from a volcanological point of view to constrain flank destabilization models and risk assessment (Boudon et al., 2007; Rosas-Carbajal et al., 2016). From a technical point of view these results allow us to validate and upgrade the original designs of our instruments (Lesparre et al., 2011) and various upgrades (Marteau et al., 2014; Jourde et al., 2016a).

Structural muography imaging has also been performed on two different volcanoes: Mt. Etna in Sicily (Carbone et al., 2013) and the Mayon in the Philippines in collaboration with EOS Singapore and PHIVOLCS (https://earthobservatory.sg/project/muon-tomography-mayon-volcano-philippines-toward-better-understanding-open-vent-systems). Complementary innovative studies have been conducted by this collaboration in underground laboratories, such as the Mont-Terri in Switzerland (https://www.mont-terri.ch/fr/page-d-accueil.html). In this laboratory, devoted to the method developments in geosciences, first trials were performed to separate geological layers of close density with a joined muon-gravimetry measurement (Jourde et al., 2015b). Since the overburden acts as a “high-energy-pass filter”, it has been also possible to study the variation in time of the high-energy muon flux and its correlation with the temperature variations at the top of the atmosphere. In particular, a very promising correlation has been pointed out with brief events, referred to as sudden stratospheric warmings (SSW), where the atmosphere’s density decreases quickly, resulting in a sharp increase of the muon flux (Tramontini et al., 2019).

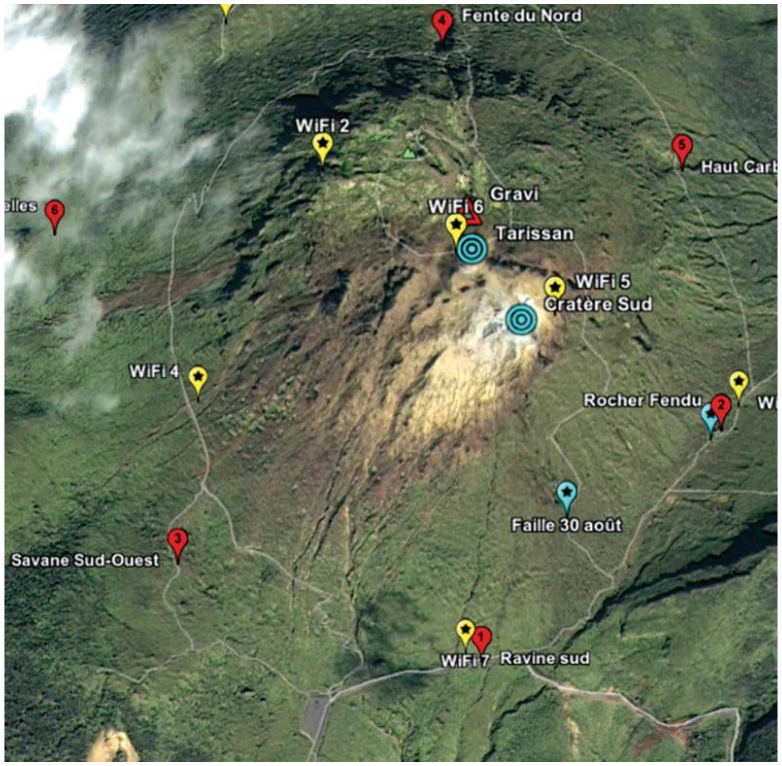

Figure 17.8 Summary of the experiments on the Soufrière of Guadeloupe with 6 muon detectors operating around the dome (red and blue symbols labelled "Savane Sud-Ouest," "Fente du Nord," "Rocher Fendu," "Faille du 30 août," "Ravine Sud"). The blue circles represent the summit stations. The yellow symbols represent the Wi-Fi relays between the telescopes and the volcano observatory where the data are stored in real time.
(Source: Google LLC)

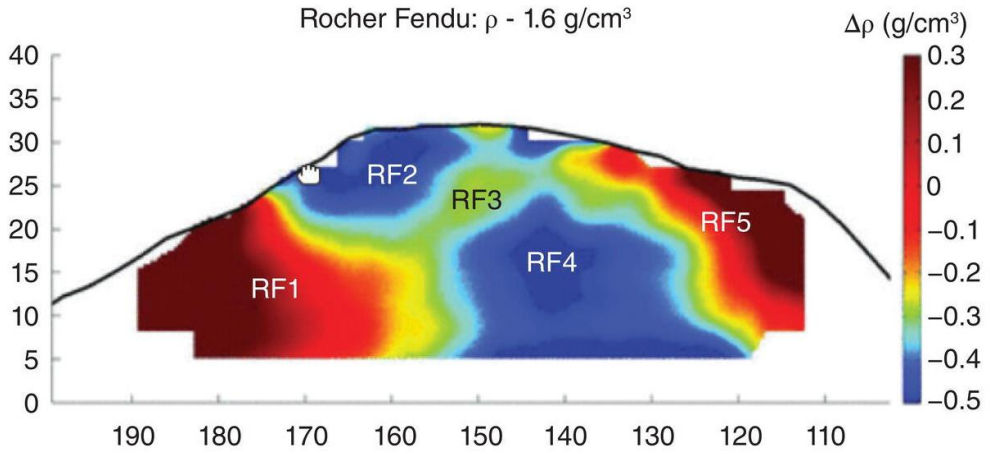

Figure 17.9 Apparent density map of the dome measured from the East side of the volcano ("Rocher Fendu" location). The blue regions correspond to negative density anomalies (low density zones) while the red regions correspond to positive density anomalies. The vertical and horizontal axis are the zenith and azimuth angles, respectively. The heteregenous structure of the dome is clear from the image, in particular just below the "South Crater" zone, the most active zone of the volcano, where vents are recorded at high velocity. Regions RF1 to RF5 correspond to zones reconstructed from the PCA analysis (Lesparre et al., 2012).

17.4. SCINTILLATORS AROUND THE WORLD

As stated earlier, scintillators have many advantages and are therefore quite popular in muography. In particular, their ease in design and operation allows their deployment in a large range of different fields. For instance, the absence of pressurized and potentially dangerous gases allow their use in regions of high risks (active volcanoes, industrial Sevezo sites), large temperature variations, low accessibility, etc. In this section, we will present some of the other collaborations running experiments using scintillators in volcanology and in other fields (archeology and industrial control). This section does not intend to be exhaustive but rather gives insight into the capabilities of scintillator-based techniques. Details may be found in various chapters of this book (see, for example, Chapter 1; Chapter 7; Chapter 9).

On volcanology, there are well-established collaborations for muon imaging of volcanoes, which led to huge progress in the understanding of the internal structure and magma dynamics. One of these is the MURAVES (MUon RAdiography of VESuvius) collaboration, aiming at the imaging of Mt. Vesuvius in Italy, one of the most dangerous and scientifically interesting volcanoes in Europe (Bonechi et al., 2017, and references therein). MURAVES is a collaboration between INGV, INFN, UCL, and UGent, and runs three detectors located on the Vesuvius slopes. This project was initiated long ago with the MURAY project of collaborative efforts around methodological and instrumentation developments (Beauducel et al., 2010). One of its interesting features is the use of triangular-shaped scintillator bars, which increase the spatial resolution by combining the data from consecutive bars (Fig. 17.10).

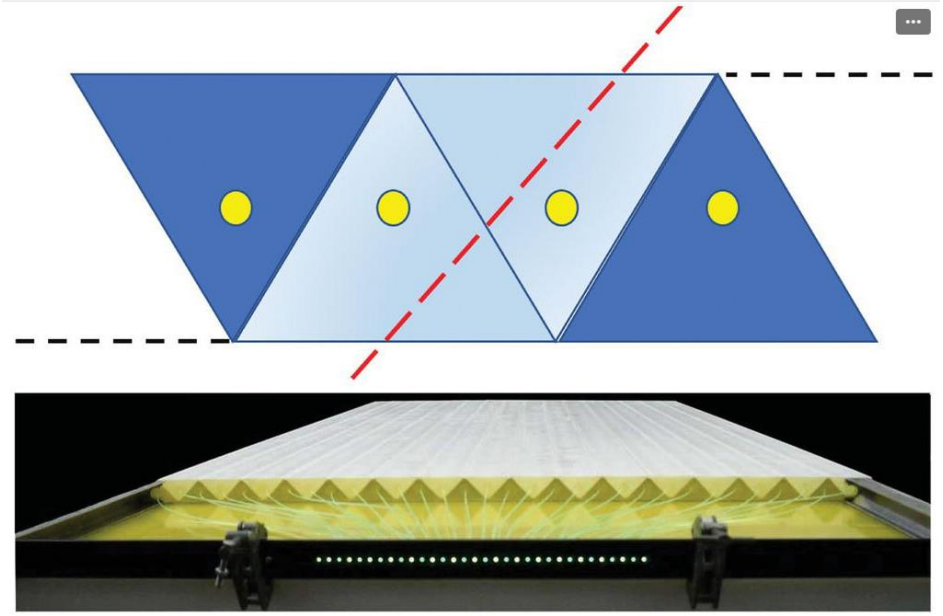

Figure 17.10 MURAVES scintillators, schematics, and detection plane. The triangular shape of the scintillator bars has been obtained by extrusion in the Fermilab laboratory. The combination of information from two adjacent bars allow an increase in spatial resolution by weighting the amount of light collected in each bar
(Bonechi et al., 2017, with permission of EDP Sciences/http://creativecommons.org/licenses/by/4.0/). Licensed under CC BY-4.0.

Italian volcanoes are well-known key targets for muography; apart from Vesuvius (Fig. 17.11), both Etna (effusive) and Stromboli (explosive) have been muographied by different techniques.

The first MURAY attempts on Vesuvius were based on the pioneering works of Prof. Tanaka using different types of scintillator detectors, from very large ones with photo-multipliers directly glued on large scintillator bars to more integrated ones (for these early works, see Tanaka et al., 2007, 2008, and 2009 references). A typical set of setup and results obtained in those early works is displayed in Fig. 17.12.

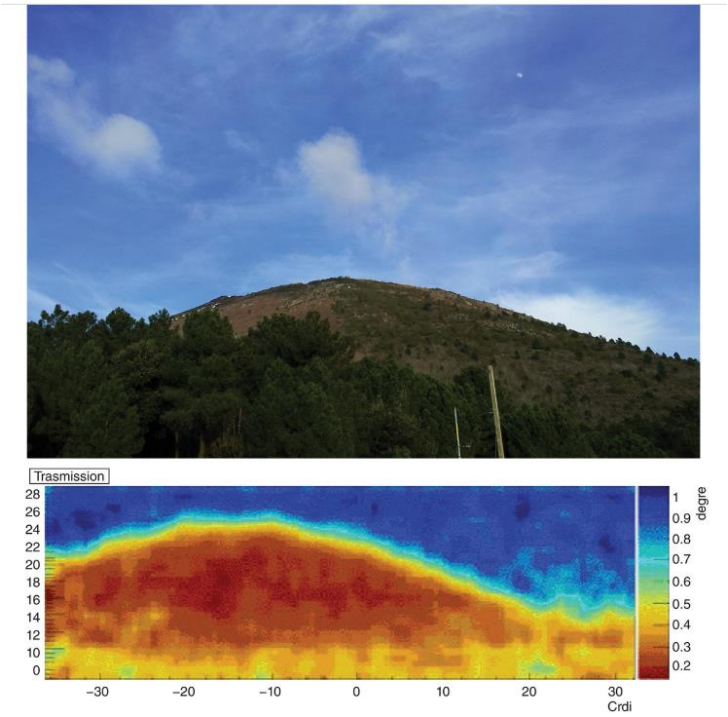

Figure 17.11 MURAVES structural imaging of the Vesuvius. The color scale has the same signification than the one of Fig. 17.9
(Bonechi et al., 2017, with permission of EDP Sciences/http://creativecommons.org/licenses/by/4.0/).

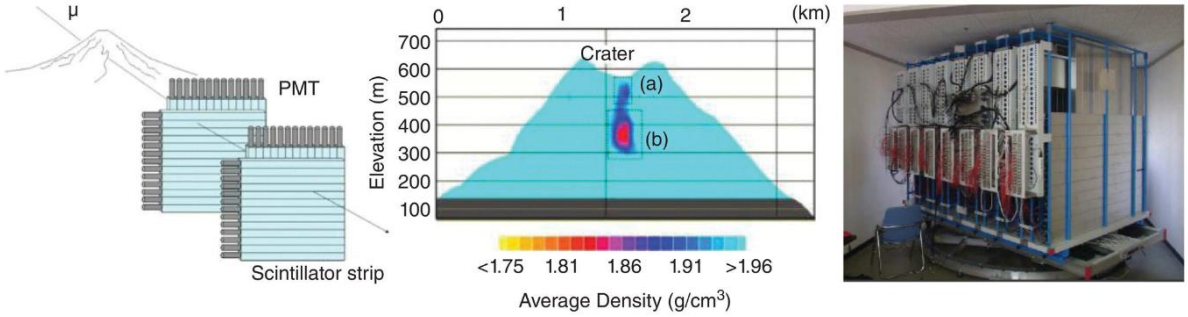

Figure 17.12(Left) Schematic view of the radiographic imaging of a volcano by scintillator detectors where photo- multipliers are directly connected to large scintillator bars. (Middle) Apparent density map of Mt. Iwodake reconstructed from the measured muon flux. The low-density anomalies, (a) and (b) originate from volcanic gases and lava (Okubo & Tanaka, 2012). (Right) Picture of a muon detector build at the Earthquake Research Institute (ERI) of the University of Tokyo
(Tanaka et al., 2014 with permission of Springer Nature/https://creatviecommons.org/licenses/by/3.0).

17.5. NON-VOLCANOLOGIC APPLICATIONS: INVESTIGATION ON NUCLEAR REACTORS AND TUNNEL-BORING MACHINES

To conclude this chapter, we would like to emphasize the adaptability of the scintillator-based muography with two examples taken outside the field of volcanology. We already mentioned in the introduction that scintillator-based detectors were successfully applied in various environments, e.g., in an Egyptian pyramid (ScanPyramids project), underground mines (Schouten & Lendru, 2018), and railway tunnels (Thompson et al., 2020). Those applications illustrate the imaging power of muography and its operability in autonomous and remote control modes.
These features make it a perfect candidate for non-invasive and non-destructive controls of large and dense industrial structures such as, e.g., nuclear power plants or blast furnaces. We will take as a first

example the investigation performed in the Fukushima Daiichi nuclear power plant in 2014–2015 (Fujii et al., 2020).
The second example is taken from the civil engineering field, where the presence of unexpected voids often signifies a weakness in material and could represent a potential danger, particularly for tunnel-boring machines (TBM).
These two examples are not exhaustive, but they give the perspectives of two typical applications of muography, one "outdoor" and the other "underground". Both suffer from their relative drawbacks: large background rejection requirements on the one hand, and low statistics on the other.

17.5.1. Nuclear Reactor Investigation

The nuclear power reactors of Fukushima Daiichi were heavily damaged by the giant earthquake and subsequent tsunami that occurred in March 2011. Before decommissioning, it was necessary to acquire information about the status of the reactors. Because of the high radiation inside and around the reactor buildings, muography techniques were used to study the situation of the reactor, specifically the status of the nuclear fuel assemblies. A scintillator-based detector system was built and calibrated at the nuclear reactor of the JAPC at Tokai, Ibaraki, Japan. This resulted in a successful imaging of the inner structure of the reactor. The detector was then brought to the Unit-1 reactor of Fukushima Daiichi and operated there from February 2014 to June 2015. The Unit-1 reactor was damaged, with its top concrete walls blown away by a hydrogen gas explosion.
The muon-tracking detectors were placed outside the reactor building. They consisted in three XY sets of 1 cm-wide plastic scintillation bar counters arranged in planes of 1 m × 1 m. The muon telescope was housed in a container of 10 cm-thick iron to suppress the effects of the environmental radiation. Indeed, one of the major concerns in operating the detector on-site at Fukushima Daiichi was the effect of the environmental radiation, which was reported to be as high as 0.5 mSv/h around the Unit-1 reactor building, requiring an iron shield thickness of 10 cm. Fig. 17.13 shows one of the muon telescope systems. The detection system was equipped with an air conditioner to provide a constant temperature inside the iron shield of 20 ± 3°C for stable operation of the photo-device, a multi-pixel photon counter (MPPC). This experimental constraint, as well as the total weight of the detector, required a well-structured environment and would not have been operated anywhere else.
The important result of this study is the success in identifying the inner structure of the reactor complex, such as the reactor containment vessel, pressure vessel, and other structures of the reactor building, through the concrete wall of the reactor building (Fig. 17.13). It was found that a large number of fuel assemblies were missing in the original fuel loading zone inside the pressure vessel. The natural interpretation is that most of the nuclear fuel melted and dropped down to the bottom of the pressure vessel, or even below.

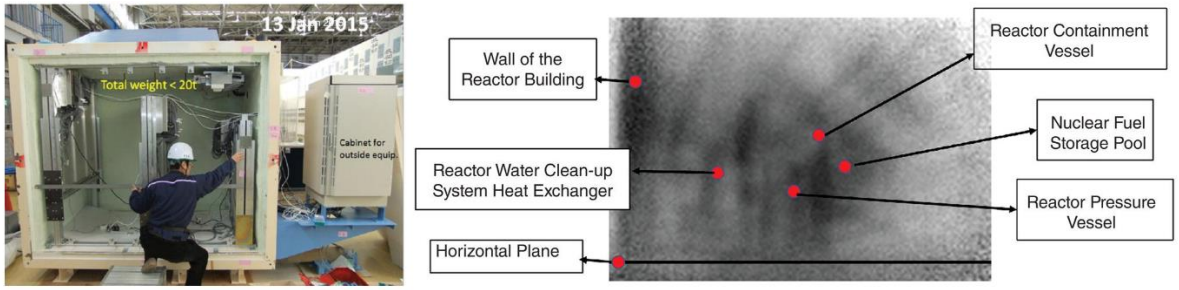

Figure 17.13 (Left) The muon telescope housed in an iron shield box made of 10 cm iron plates. The relative elevation heights of the three X–Y assemblies are adjusted to target the Unit-1 fuel loading zone. For thermal insulation, 6 cm-thick plastic foam is plastered over the inner wall of the box. The cabinet next to the box houses the air conditioner controller and data network hub for data transfer and communication with the assemblies. The total weight is 20 t. (Right) Image of the Unit-1 reactor of Fukushima Daiichi after 90 days observed by the detection system placed at the northwestern corner of the reactor building (Fujii et al., 2020, with permission of Oxford University Press/https://creativecommons.org/licenses/by/4.0).

Figure 17.14 (Left) Picture of a Tunnel-boring Machine (TBM) of the Herrenknecht company, one of the world's leader in the field during its construction phase
(Source: ©Scottish Plant, https://www.scottishplant.co.uk/heres-a-boring-story/).
(Right) Artistic view of a TBM while digging an urban tunnel
(Source: ©Medium.com https://medium.com/netive-in/17th-tunnel-boring-machine-lowered-for-metro-iii-tunnel-work-1c5f7360af29).

17.5.2. Tunnel-Boring Machines

Tunnel-boring projects require a considerable amount of planning, well ahead of drilling operations. Despite these precautionary measures, unexpected ground geological features (local density variations, cavities, unstable superficial ground, instabilities induced by the driller) impose real-time, possible expensive, adaptations to the drilling operations.
The direct relation of muon flux absorption with the density of a given medium makes muography a promising solution to provide a real-time density analysis of geological objects in front of the tunnel-boring machine (TBM). A picture of such a TBM is displayed in Fig. 17.14 (left). An artistic view of the TBM digging operation is displayed on the right of Fig. 17.14.
To test its applicability during the drilling of the "Grand Paris Express" subway network, a muon telescope was used in two different experiments. The muon detector is one from the Diaphane collaboration, used on the Soufrière of Guadeloupe. First it was placed beside the TBM, directed towards the drilled cylinder from a lateral perspective. Then it was moved directly inside the TBM for the rest of the drilling operation (left of Fig. 17.15).
These experiments provide a unique dataset to optimize the methodology. Because the telescope is moving forward, the muon flux crossing a particular geological object measured by the telescope has different directions with respect to time, allowing 3D density estimates. An example of apparent density 3D reconstruction distribution of the ground, using inhomogeneous Poisson likelihood, is presented in Fig. 17.15. The algorithms for this particular reconstruction remove systematic noise from the buildings; caves, etc., are patented.

17.6. CONCLUSIONS

This chapter presented general features of scintillator-based detectors used for muography. The key properties of scintillators that make them suitable for a large number of applications, from Earth Sciences to non-invasive and non-destructive controls in the industry, are their relatively fast signals (∼ns), their high muon detection efficiency, and the ease of design. Their major limitations are their mass, which in return improves their robustness. The portability of those detectors, as well as their spatial resolution, are directly derived from the design itself (transverse segmentation, bars width, total surface, etc.). Thanks to their relatively fast signal production, scintillators are applicable for time-of-flight measurement of particles across the tracking system and thus discriminate the upward- and downward-going particles. The photo-detectors used to read out the scintillation photons (after potential shifting in the spectral range) can work in wide temperature ranges with quite low power consumption. All these features make those detectors ideal tools for feasibility studies on unknown and harsh environments. They are at present the most popular detectors used in muography.

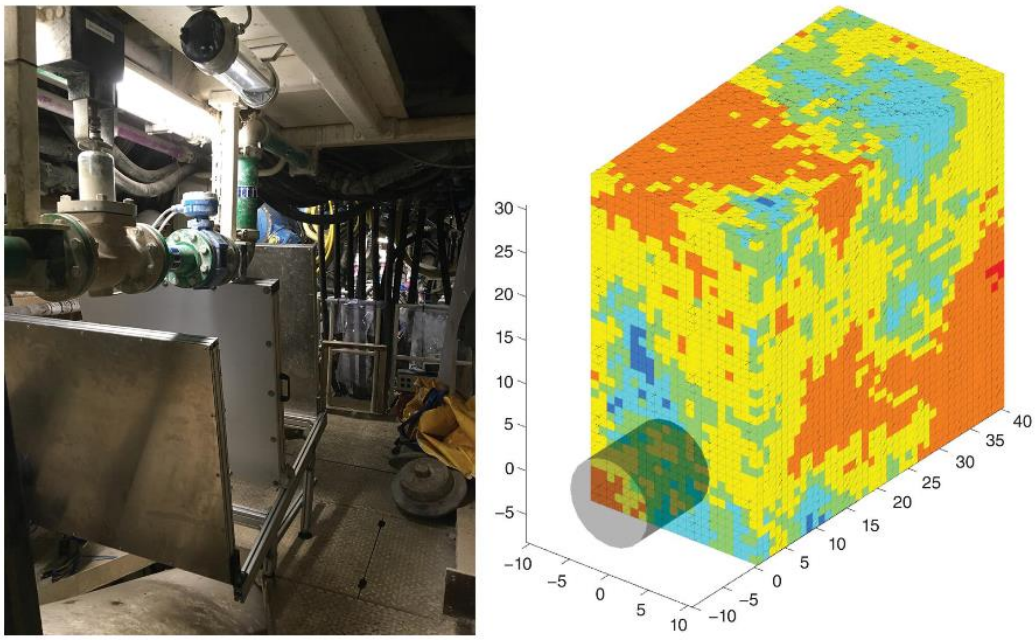

Figure 17.15 (Left) Picture of the muon detector inside the TBM. (Right) Example of online 3D apparent density reconstruction averaging the last 50 meters of the TBM movement
(credits J.Marteau, IP2I, CNRS/IN2P3, Université de Lyon)

ACKNOWLEDGMENTS

One of the authors (J.M.) wants to address a warm and special thanks to Christel and Fabrice Dufour for their essential help on the field and their irreplaceable friendship. This work is dedicated to the memory of Fabrice.

REFERENCES

Abe, K., Abgrall, N., Aihara, H., Akiri, T., Albert, J.B., Andreopoulos, C., et al. (T2K Collaboration) (2013). Evidence of electron neutrino appearance in a muon neutrino beam. Physical Review D, 88(3), 032002. https://doi.org/10.1103/PhysRevD.88.032002

Adamson, P., Andreopoulos, C., Arms, K.E., Armstrong, R., Auty, D.J., Ayres D.S., et al. (MINOS Collaboration). (2008). Measurement of neutrino oscillations with the MINOS detectors in the NuMI beam. Physical Review Letters, 101(13), 131802. https://doi.org/10.1103/PhysRevLett.101.131802

Agafonova, N., Aleksandrov, A., Altinok, O., Ambrosio, M., Anokhina, A., Aoki, S., et al. (OPERA Collaboration). (2010). Observation of a first ντ candidate in the OPERA experiment in the CNGS beam. Physics Letters B, 691, 138–145. https://doi.org/10.1016/j.physletb.2010.06.022

Alvarez, L. W., Anderson, J. A., Bedwei, F. E., Burkhard, J., Fakhry, A., Girgis, A., et al. (1970). Search for hidden chambers in the Pyramids. Science, 167, 832839. https://doi.org/10.1126/science.167.3919.832

Beauducel, F., Bross, A., Buontempo, S., D'Auria, L., Déclais, Y., De Lellis, G., et al. (2010). The MU-RAY project: Summary of the round-table discussions. Earth Planets and Space, 52, 145–151. https://doi.org/10.5047/eps.2009.03.004

Bonechi, L., Ambrosino, F., Cimmino, L., D'Alessandro, R., Macedonio, G., Melon, B., et al. (2017). The MURAVES project and other parallel activities on muon absorption radiography. The European Physical Journal Conferences. 02015. https://doi.org/10.1051/epjconf/201818202015

Boudon, G., Le Friant, A., Komorowski, J.-C., Deplus, C., & Semet, M. (2007). Volcano flank instability in the Lesser Antilles arc: diversity of scale, processes, and temporal recurrence. Journal of Geophysical Research: Solid Earth, 112(B8). https://doi.org/10.1029/2006JB004674

Carbone, D., Gibert, D., Marteau, J., Diament, M., Zuccarello, L., & Galichet, E. (2013). An experiment of muon imaging at Mt. Etna (Italy), Geophysics Journal International, 196(2), 633–643. GJI-13-0406. https://doi.org/10.1093/gji/ggt403

Fujii, H., Hara, K., Hayashi, K., Kakuno, H., Kodama, H., Nagamine, K., et al. (2020). Investigation of the Unit-1 nuclear reactor of Fukushima Daiichi by cosmic muon radiography. Progress of Theoretical and Experimental Physics, 2020(4), 043C02. https://doi.org/10.1093/ptep/ptaa027

Gaisser, T. K., Engel, R., & Resconi, E. (2016). Cosmic Rays and Particle Physics. Cambridge: Cambridge University Press.

Gómez, H., Gibert, D., Goy, C., Jourde, K., Karyotakis, Y., Katsanevas, S., et al. (2017). Forward scattering effects on muon imaging. Journal of Instrumentation, 12(12), P12018. https://doi.org/10.1088/1748-0221/12/12/P12018

Jourde, K., Gibert, D., Marteau, J., de Bremond d'Ars, J., Gardien, S., Girerd, C., et al. (2013). Experimental detection of upward going cosmic particles and consequences for correction of density radiography of volcanoes. Geophysical Research Letters, 40(24), 6334–6339. https://doi.org/10.1002/2013GL058357

Jourde, K., Gibert, D., & Marteau, J. (2015a). Improvement of density models of geological structures by fusion of gravity data and cosmic muon radiographies. Geoscientific Instrumentation, Methods and Data Systems, 4, 177–188. https://doi.org/10.5194/gi-4-177-2015

Jourde, K., Gibert, D., & Marteau, J. (2015b). Joint inversion of muon tomography and gravimetry - a resolving kernel approach. Geoscientific Instrumentation, Methods and Data Systems Discussions, 5, 83–116. https://doi.org/10.5194/gid-5-83-2015

Jourde, K., Gibert, D., Marteau, J., de Bremond d'Ars, J., Gardien, S., Girerd, C., & Ianigro, J.-C. (2016a). Monitoring temporal opacity fluctuations of large structures with muon radiography: a calibration experiment using a water tower. Scientific Reports, 6(1), 1–11. https://doi.org/10.1038/srep23054

Jourde, K., Gibert, D., Marteau, J., de Bremond d'Ars, J., & Komorowski, J.-C. (2016b). Muon dynamic radiography of density changes induced by hydrothermal activity at the La Soufrière of Guadeloupe volcano. Scientific Reports, 6, 33406. https://doi.org/10.1038/srep33406

Le Gonidec, Y., Rosas-Carbajal, M., de Bremond d'Ars, J., Carlus, B., Ianigro, J.-C., Kergosien, B., et al. (2019). Abrupt changes of hydrothermal activity in a lava dome detected by combined seismic and muon monitoring. Scientific Reports, 9(1), 1–9. https://doi.org/10.1038/s41598-019-39606-3

Leo, W. R. (1987). Techniques for Nuclear and Particle Physics Experiments: A How to Approach. Springer. 368 p, ISBN: 9783540572800.

Lesparre, N., Gibert, D., Marteau, J., Déclais, Y., Carbone, D., & Galichet, E. (2010). Geophysical muon imaging: feasibility and limits. Geophysical Journal International, 183(3), 1348–1361. https://doi.org/10.1111/j.1365-246X.2010.04790.x

Lesparre, N., Marteau, J., Déclais, Y., Gibert, D., Carlus, B., Nicollin, F., & Kergosien, B. (2011). Design and operation of a field telescope for cosmic ray geophysical tomography. Geoscientific Instrumentation Methods and Data Systems, 1(1), 47–89. https://doi.org/10.5194/gi-1-33-2012

Lesparre, N., Gibert, D., Marteau, J., Komorowski, J.-C., Nicollin, F., & Coutant, O. (2012). Density muon radiography of La Soufrière of Guadeloupe volcano: comparison with geological, electrical resistivity and gravity data. Geophysics Journal International, 190, 1008–1019. https://doi.org/10.1111/j.1365- 246X.2012.05546.x

Marteau, J., Gibert, D., Lesparre, N., Nicollin, F., Noli, P., & Giacoppo, F. (2012). Muons tomography applied to geosciences and volcanology. Nuclear Instruments and Methods in Physics A, 695, 23–28. https://doi.org/10.1016/j.nima.2011.11.061

Marteau, J., de Bremond d'Ars, J., Gibert, D., Jourde, K., Gardien, S., Girerd, C., & Ianigro, J.-C. (2014). Implementation of sub-nanosecond time-to-digital convertor in field-programmable gate array: applications to time-of-flight analysis in muon radiography. Measurement Science and Technology, 25(3), 035101. https://doi.org/10.1088/0957-0233/25/3/035101

Morishima, K., Kuno, M., Nishio, A., Kitagawa, N., Manabe, Y., Moto, M., et al. (2017). Discovery of a big void in Khufu's Pyramid by observation of cosmic-ray muons. Nature, 552, 386–390. https://doi.org/10.1038/nature24647

Nagamine, K. (2003). Introductory Muon Science. Cambridge: Cambridge University Press.

Okubo, S., & Tanaka, H. K. M. (2012). Imaging the density profile of a volcano interior with cosmic-ray muon radiography combined with classical gravimetry. Measurement Science and Technology, 23(2012), 042001. https://doi.org/10.1088/0957-0233/23/4/042001

Pla-Dalmau, A., Bross, A. D. & Mellott, K. L. (2001). Low-cost extruded plastic scintillator. Nuclear Instruments and Methods in Physics Research Section A, 466, 482–491. https://doi.org/10.1016/S0168-9002(01)00177-2

Rosas-Carbajal, M., Komorowski, J.-C., Nicollin, F., & Gibert, D. (2016). Volcano electrical tomography unveils edifice collapse hazard linked to hydrothermal system structure and dynamics. Scientific Reports, 6, 29899. https://doi.org/10.1038/srep29899

Rosas-Carbajal, M., Jourde, K., Marteau, J., Deroussi, S., Komorowski, J.-C., & Gibert, D. (2017). Three-dimensional density structure of la soufrière de Guadeloupe lava dome from simultaneous muon radiographies and gravity data. Geophysical Research Letters, 44(13), 6743–6751. https://doi.org/10.1002/2017GL074285

Schouten, D. W., & Ledru, P. (2018). Muon tomography applied to a dense uranium deposit at the McArthur River mine. Journal of Geophysical Research: Solid Earth, 123, 8637–8652. https://doi.org/10.1029/2018JB015626

Sullivan, J. D. (1971). Geometrical factor and directional response of single and multi-element particle telescopes. Nuclear Instruments and Methods, 95, 5–11. https://doi.org/10.1016/0029-554X(71)90033-4

Tanaka, H. K. M., Nakano, T., Takahashi, S., Yoshida, J., Takeo, M., Oikawa, J., et al. (2007). High resolution imaging in the inhomogeneous crust with cosmic-ray muon radiography: The density structure below the volcanic crater floor of Mt. Asama, Japan. Earth and Planetary Science Letters, 263, 104–113. https://doi.org/10.1016/j.epsl.2007.09.001

Tanaka, H. K. M., Nakano, T., Takahashi, S., Yoshida, J., Takeo, M., Oikawa, J., et al. (2008). Radiographic imaging below a volcanic crater floor with cosmic-ray muons. American Journal of Science, 308(7), 843–850. https://doi.org/10.2475/07.2008.02

Tanaka, H. K. M., Uchida, T., Tanaka, M., Takeo, M., Oikawa, J., Ohminato, T., et al. (2009). Detecting a mass change inside a volcano by cosmic-ray muon radiography (muography): First results from measurements at Asama volcano, Japan. Geophysical Research Letters, 36, L17302. https://doi.org/10.1029/2009GL039448

Tanaka, H., Kusagaya, T. & Shinohara, H. (2014) Radiographic visualization of magma dynamics in an erupting volcano. Nature Communications, 5, 3381. https://doi.org/10.1038/ncomms4381

Thompson, L. F., Stowell, J. P., Fargher, S. J., Steer, C. A., Loughney, K. L., O'Sullivan, E. M., et al. (2020). Muon tomography for railway tunnel imaging. Physical Review Research, 2, 023017. https://doi.org/10.1103/PhysRevResearch.2.023017

Tramontini, M., Rosas-Carbajal, M., Nussbaum, C., Gibert, D., & Marteau, J. (2019). Middle-atmosphere dynamics observed with a portable muon detector. Earth and Space Science, 6(10). https://doi.org/10.1029/2019EA000655.